#1 Francisco J Escobedo (Referee)

Comment #1-1
MS No. essd-2019-9: A dataset of 30-meter annual vegetation phenology indicators (1985-2015) in urban areas of the conterminous United States. Below is my review for the above manuscript. Overall, I found it novel and a contribution to future research on the ecology of urban and peri-urban ecosystems in the United States. I have included some grammar and context suggestions as well as other suggestions. Key among these is that this data set can have many more applications that the ones currently presented in the manuscript. I have included some of these suggestions.

Response: thank you for your positive comments. We addressed your concerns and made corresponding revisions. Details can be found in our attached response letter.

Comment #1-2
In terms of data quality, I did view some scenes directly on the Figshare site and did notice some problems with the overall visual quality of the scenes as many were distorted and banded. I also downloaded and opened in ArcCatalog and ArcMap some of the raster datasets. I did have a difficult time in trying to determine the overall content and geographic location of many of the images. The SHP file did help but a summary and description of each raster data set might have been helpful. However, I did not open every single raster data set or overlay some of these onto other geospatial data to assess their quality.

Response: we appreciate your suggestions for our dataset. The visualization of thumbnails in FigShare is not accurate due to its small size. The distorted and banded regions do not exist when visualizing the data in professional software such as ArcMap and Matlab. We provided a detailed example to explain this issue. As suggested, we also added a field of "CityName" in our provided SHP file, which helps to locate the region of each scene quickly. For each scene, we offered a COR layer for the fitting performance of the double logistic model. This helps users understand the uncertainty of the derived phenology indicator at the pixel level. Accordingly, we updated our data descriptions in FigShare. We provided a more detailed explanation of our dataset in the response to comment #1-17.

Below are some comments regarding the manuscript, which I hope you will find useful.

Comment #1-3
Abstract Page, (P) 2, Line (L) 10 and P3, L2: I would think that currently "fine-resolution" refers to sub meter imagery. Landsat may have been fine in the 1980-90s but now it is considered medium resolution I would think.

Response: agree. We revised it in our manuscript. Below are two examples.

*"**Medium**-resolution satellite observations show great potential for characterizing seasonal and annual dynamics of vegetation phenology in urban domains" (page 1, line 10).*

*"The derived phenology product in the US urban domains at the national level is of great use for urban ecology studies for its **medium** spatial resolution (30 m) and long temporal span (30 years)" (page 2, line 1).*

Comment #1-4
P2, L 10-14: Atmospheric, soil and light pollution in urban environments will also drive plant phenology (e.g., leaf deciduousness-senescence), such a dataset can have applications to address issues like these.

Response: thank you. We added potential applications of our dataset in urban environments as suggested.

"Changes in the urban environment due to atmospheric, soil, and light pollutions will affect plant phenology (e.g., leaf senescence) (Escobedo et al., 2011), resulting in different phenology characteristics in urban ecosystems" (page 2, line 14).

> Escobedo, F.J., Kroeger, T., & Wagner, J.E. (2011). *Urban forests and pollution mitigation: Analyzing ecosystem services and disservices. Environmental Pollution, 159, 2078-2087.*

Comment #1-5
P2, L 15: Urban morphology might be more relevant than "development"

Response: done.

Comment #1-6
P3, L5, "There have been" few attempts. . . Also specify what you mean here by "large scale". I believe you mean something like "regional (as opposed to local) scale".

Response: yes. We clarified this sentence as below.

*"There are few attempts of mapping vegetation phenology in urban domains using Landsat observations at a **regional (or global) scale** due to complex vegetation compositions in urban ecosystems and the large dataset required for analysis" (page 3, line 7).*

Comment #1-7
P3, L13, ". . .therefore lack large-scale. . ."

Response: done.

Comment #1-8
P3 L14, ". . .urban ecosystem are more complex. . ." Mention something about the high floral species richness found in cities, relative to rural area in these latitudes.

Response: thank you. We discussed the difference of species richness in cities and rural areas.

"vegetation types and compositions in urban ecosystems are more complicated, and the floral species are more abundant in cities than surrounding rural areas (Luz de la Maza et al., 2002)" (page 3, line 16).

> Luz de la Maza, C., Hernández, J., Bown, H., Rodríguez, M., & Escobedo, F. (2002). *Vegetation diversity in the Santiago de Chile urban ecosystem. Arboricultural journal, 26, 347-357.*

Comment #1-9
P4, L9: Perhaps say urban areas instead of cities.

Response: done.

Comment #1-10
P4L 10: You did not use Landsat for the NTL observation I imagine?

Response: Yes, we derived urban extents from NTL observations (Zhou et al., 2018).

> Zhou, YY., Li, XC., Asrar, G, Smith, S, & Imhoff, M. (2018). *A global record of annual urban dynamics (1992-2013) from nighttime lights. Remote Sensing of Environment, 219, 206-220.*

Comment #1-11
P4 L 18-19: Specify all the correction procedures (e.g., cloud removal) used.

Response: thank you. We specified correction procedures used in Landsat images.

"The correction of atmospheric effect was performed using the Landsat ecosystem disturbance adaptive processing system (LEDAPS) (Masek et al., 2006), and clouds and shadows were removed using the function of mask procedure (Fmask) (Zhu and Woodcock, 2012) before compositing the EVI time series" (page 4, line 21).

Comment #1-12

P6 L 1-5: As mentioned in the introduction, urban area are heterogeneous and complex, in terms of not only vegetation diversity and phenology, but land use/covers as well. How was this accounted for in your methods? That is "vegetation" and "urban areas" are not homogenous in terms of their spectral and environmental characteristics. Land cover change is mentioned in Line 5 but did you develop a new, or use an existing urban land cover classification?

Response: thank you for your questions. We did not separately calculate phenology indicators before and after land use cover change because we used the long-term Landsat time series data to derive the mean phenology pattern. This could introduce the uncertainty in our result in areas with land cover changes. The uncertainties caused by such changes can be detected in the fitting performance of the double logistic model. These changed pixels can be excluded for specific applications by users. We clarified this in our revised manuscript as follows:

"sigmoid curves during green-up and senescence phrases are notably different across different vegetation cover types (e.g., forest and cropland). We evaluated the performance of the fitted double logistic model based on the correlation between the fitted and observed EVI observations. Pixels with land use/cover change during the study period or weak vegetation signals (e.g., extremely high built-up area or barren land) could have a low fitting performance, and these pixels can be excluded for specific applications." (page 6, line 6).

Comment #1-13

P8 L 24-25: Was the fact that these appear exclusively to be deciduous forest types a coincidence? Specifically, how do evergreen forest types/trees affect the urban phenology results?

Response: thank you for the questions. Yes. The dominant vegetation type in Harvard forest is the deciduous forest. For other vegetation types like the evergreen forest, the performance of our derived phenology results depends on the ability of the remote sensing signal to capture their reflectance signature. As shown in Fig. 4 (site 1), we observed a clear phenology pattern in Site 1 (Florida), where the evergreen forest is the dominated vegetation type. For regions (e.g., grassland) with relatively low performance, they can be indicated in the associated uncertainty in our dataset. We further explained this in the revised manuscript.

"Three dominant species of deciduous forest in the HF, including the red oak (Quercus rubra; QURU), red maple (Acer rubrum; ACRU), and yellow birch (Betula alleghaniensis; BEAL), were used in our analysis. However, for other vegetation types (e.g., evergreen forest), discernible phenology patterns can be also captured using the proposed methodology (e.g. Fig. 4, Site 1)." (page 9, line 8).

Comment #1-14

P10 L10-11: Can increased impervious surfaces, pollution or changing species composition over the analysis period, also be a correlate?

Response: thank you for your question. We clarified it in our revised manuscript.

"In addition, changes in urban environment such as impervious surface, air pollution, and species compositions can affect the spatiotemporal pattern of vegetation phenology in urban ecosystems (Li et al., 2015; Escobedo et al., 2011)" (page 10, line 24).

Comment #1-15

Conclusion: the first two paragraphs are repetitive. Perhaps discuss some limitations and more applications e.g., many vegetation-air pollution deposition models need leaf on/off data, city-level urban tree cover classification need to be done during leaf on, etc.

Response: thank you for your suggestions. The first paragraph summarizes the main steps we used to obtain our results and the second one presents evaluations of our dataset in comparison with other products. Thus, we would prefer to keep the current form of these two paragraphs. As suggested, we added discussion of limitations and potential applications of our dataset in urban studies.

"In addition, the derived leaf on/off information in this dataset is potentially useful for vegetation-air pollution deposition models (Escobedo and Nowak, 2009). However, it is worth noting that this dataset is most applicable for deciduous forest type. For grassland and evergreen forests in tropical areas, the uncertainty could be high in the derived phenology indicators. In addition, our phenology algorithm did not specifically consider pixels with land cover changes, which could be further improved when the product of annual urban dynamics becomes available." (page 12, line 7).

  ➢ *Escobedo, F.J., & Nowak, D.J. (2009). Spatial heterogeneity and air pollution removal by an urban forest. Landscape and Urban Planning, 90, 102-110.*

Comment #1-16
Figure 1-11 A1. Please spell out all acronyms. The reader should not have to read the text to find what the acronyms and symbols are.

Response: thank you. We spelled out all acronyms in the revised figures.

Comment #1-17
Data quality from: https://doi.org/10.6084/m9.figshare.7685645.v2. I viewed thumbnails of all the *.tif files but did not attempt to download all since I am having trouble with memory and the ArcGis license. I did download and view several files and viewed them in the figshare site. Some of these scenes in the figsahre.com site (e.g., US_uCluster_83_COR-1985-2015.tif) seemed to have distortion in the form of a distorted scene, specifically 1/3 of the image was banded and distorted. I did view several other raster data sets in ArcCatalog (e.g. The uCluster_USA_gt500) and a summary and descriptions in the "Description" or metadata of the Raster dataset would have been helpful in understanding the content data set. The uCluster_USA_gt500. However, I am unable to fully assess data quality at this time.

Response: we appreciate your efforts to examine our dataset and your suggestions. We noticed that FigShare has some problems in thumbnails. Below is an example of the image "US_uCluster_83_COR-1985-2015" in FigShare and ArcMap. These banded and distorted areas in FigShare does not exist in ArcMap. We also found similar issues in other scenes in FigShare thumbnails. We explained this in the data description for awareness of the users. We also added a new field of region/city name in the provided shapefile of uCluster_USA_gt500, to help locate the region of interest using the information of cityName.
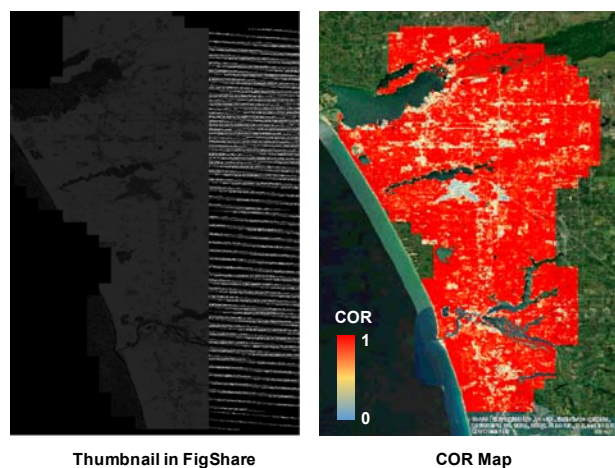

Fig. R1. An illustration of COR images visualized in FigShare (left) and ArcMap (right).

#2 Yongshuo Fu (Referee)

Comment #2-1

Li and coauthors produced a 30-meter phenology dataset using Google earth engine based Landsat images, and a double logistic model. The study is timely and important. The fine-resolution phenology dataset is valuable, and provide an avenue on the urban phenology study since its high importance in public health, i.e. pollen allergy diseases, as well as urban ecosystem response to future climate warming. I would thus like to recommend publishing this nice study in the ESSD. Below, please find some suggestions that I hope can be help to improve the MS.

Response: thank you for your positive feedback. Below please find our detailed response to each comment.

Comment #2-2

First, the authors argued that the logistic model is valuable to capture the trends of green-up and senescence by using the pair-parameters, but the description is weaker. Please specify or update this. In addition, the half-maximum criterion was used to extract the SOS and EOS, but the more popular method is using the maximum change rate. Different methods might generate different results, see the figure 10, between the MODIS EVI and MCD12Q2, and large difference was obtained. I do not say the half-maximum is wrong, but the authors should address this issue in the discussion, and remind the reader to cite the method when using the dataset.

Response: thank you for your suggestion. We clarified the double logistic model in the revised manuscript.

"That is, n_1 and n_2 are dates with the maximum increasing and decreasing rates of green-up and senescence in sigmoid curves, while m_1 and m_2 are slopes that determine the shape of sigmoid curves" (page 5, line 24).

The half-maximum criterion (i.e., middle of the sigmoid curve) determines the dates with the maximum increasing and decreasing rates of the first derivative (i.e., change rate) in EVI (Fisher et al., 2006). This method was applied to the Landsat and MODIS EVI data. While for the phenology product of MCD12Q2, SOS and EOS are the dates at the base of the sigmoid curve (i.e., the inflection point). Thus, the derived SOS using our method is later than MCD12Q2 while EOS is earlier than MCD12Q2. We clarified this in the revised manuscript.

"We derived phenology indicators of SOS and EOS using a half-maximum criterion method (Fisher et al., 2006). In this method, SOS and EOS were calculated as dates when the first derivative of EVI reaches the maximum increasing and decreasing rates during the green-up and senescence phases, respectively. Although there are other definitions of SOS and EOS such as inflection points (i.e., at the base of sigmoid curve) (Zhang et al., 2003), the criterion used in the study is more temporally stable and can be applied to plants with different canopy structures (Fisher and Mustard, 2007)" (page 6, line 14).

"It is worth noting that SOS derived from the half-maximum criterion in this study is consistently later compared to the MODIS product using the criterion of the inflection point" (page 10, Line 13).

Comment #2-3

Second, the Landsat phenology dataset was compared with in situ phenology data, including both phenoCam and ground observations, and I found the authors overestimated the results, i.e. a good agreement between these datasets. See the figure 6 and 7, the difference between Landsat and phenoCam is even larger than 20 days, i.e., RMSEs, for both SOS and EOS. Actually, I do not expect a high agreement, due to the forest structure and the difference of scale between Landsat (30m) and in situ observations (500m for PhenoCam). Therefore, I would suggest updating the descriptions of these comparisons, and highlighting the scale issues between the Landsat and PhenoCam and ground dataset.

Response: thank you for your suggestion. We agreed that the difference between Landsat and *in-suit* derived phenology results is mainly attributed to the scale effect of these two datasets, as well as the difference in background vegetation types and used vegetation indices. We revised our description of data comparison (i.e., removing phrases like "good agreement") and discussed these factors in our revised text.

"For those sites (blue or light blue dots) with large differences, the performance of fitting Landsat EVIs using the double logistic model is relatively low because these sites are mainly embedded in ecosystems that are dominated by shrubs, evergreen forests, or wetlands (Fig. S3)" (page 8, line 4).

"Discrepancies between these two sets of phenology indicators derived from Landsat and PhenoCam are mainly attributed to factors such as: (1) two different vegetation indices (i.e., EVI and GCC); and (2) the scale effect between in-situ PhenoCam and Landsat observations (Liu et al., 2017)" (page 8, line9).

"Overall, the derived phenology indicators (SOS and EOS) are spatially consistent with those from in-situ PhenoCam data at the national scale (Fig. 6)" (page 7, line 21).

Below are some minor comments

Comment #2-4
Page 5, line 15, the physical meaning of parameter is related to vegetation growth and senescence, please specify;

Response: thank you for your suggestion. We clarified these parameters in our revised manuscript.

"where $f(t)$ is the fitted EVI value at the day t; v_1 and v_2 are the background and amplitude of EVI over the entire year, respectively; and m_1 & n_1, m_2 & n_2 are the pair-parameters that capture the trend of green-up and senescence phases of vegetation growth. That is, n_1 and n_2 are dates with the maximum increasing and decreasing rates of green-up and senescence sigmoid curves, and m_1 and m_2 are the slopes that determine the shape of two sigmoid curves" (page 12, line 17).

Comment #2-5
Page 6, line 10-15, why the half-maximum criterion is likely to produce the SOS and EOS when leaves are likely to emerge? Remove this argument or update.

Response: we removed this sentence in the revised manuscript as suggested.

Comment #2-6
Page 7, 4.1 section, the authors argued the urban-rural gradient, but in the following the forest was presented as example. Better remove this gradient arguments.

Response: thank you for your suggestion. Forest is an example for illustrating latitudinal difference of vegetation phenology in the eastern United States (Fig. 4), while for the method performance in urban ecosystems, we selected different sites (with different vegetation covers) from urban core to rural areas for illustration (Fig. 5). As suggested, we removed "urban-rural gradient".

"The performance of the developed GEE-based double logistic model is reasonably good across different latitudes and different vegetation types in urban ecosystems" (page 7, line 12).

"At the city scale, the proposed double logistic model shows a good performance of fitting EVI time series from urban to rural areas (Fig. 5)" (page 7, line 15).

Comment #2-7
Page 8, the argument in line 6, i.e. a good agreement with in-situ phenocam results, is in conflict with the line 15, i.e. the agreement is relatively weaker. Please improve these arguments.

Response: thank you for your suggestion. We clarified it in the revised manuscript.

"Overall, the annual variability of SOS derived from Landsat observations is consistent with that from the in-situ PhenoCam observations (Fig. 7)" (page 8, line 12).

Comment #2-8
Fig3, specify GLP in the legend;

Response: GLP is the abbreviation of "generalized Landsat phenology". We clarified it in the figure caption.

"Fig. 3. Illustration of the generalized Landsat phenology (GLP) approach for identifying the annual variability of phenology indicators."

#3 Dongdond Kong

Comment #3-1
Amazing work. Do you mind to publish the corresponding GEE script?
Response: thank you. We are pleased to share upon request the script for research and education by the academic community.

A dataset of 30-meter annual vegetation phenology indicators (1985-2015) in urban areas of the conterminous United States

Xuecao Li[1], Yuyu Zhou[*1], Lin Meng[1], Ghassem R. Asrar[2], Chaoqun Lu[3], Qiusheng Wu[4]

[1]Department of Geological and Atmospheric Sciences, Iowa State University, Ames, IA, 50011, USA

[2]Joint Global Change Research Institute, Pacific Northwest National Lab, College Park, MD, 20740, USA

[3]Department of Ecology, Evolution, and Organismal Biology, Iowa State University, Ames, IA, 50011, USA

[4]Department of Geography, ~~Binghamton University, SUNY~~University of Tennessee, ~~Binghamton~~Knoxville, ~~NY~~TN, ~~13902~~37996, USA

Correspondence to: Yuyu Zhou (yuyuzhou@iastate.edu)

Abstract. ~~Fine~~Medium-resolution satellite observations show great potential for characterizing seasonal and annual dynamics of vegetation phenology in urban domains, from local to regional and global scales. However, most previous studies were conducted using coarse ~~or moderate~~ resolution data, which are inadequate for characterizing the spatiotemporal dynamics of vegetation phenology in urban domains. In this study, we produced an annual vegetation phenology dataset in urban ecosystems for the conterminous United States (US), using all available Landsat images on the Google Earth Engine (GEE) platform. First, we characterized the long-term mean seasonal pattern of phenology indicators of the start of season (SOS) and the end of season (EOS), using a double logistic model. Then, we identified the annual variability of these two phenology indicators by measuring the difference of dates when the vegetation index in a specific year reaches the same magnitude as its long-term mean. The derived phenology indicators agree well with *in-situ* observations from PhenoCam network and Harvard Forest. Comparing with results derived from the moderate resolution imaging spectroradiometer (MODIS) data, our Landsat derived phenology indicators can provide more spatial details. Also, we found the temporal trends of phenology indicators (e.g., SOS) derived from Landsat and MODIS are consistent overall, but the Landsat derived results from 1985 ~~have~~offer a longer temporal span compared to MODIS from 2001 to present. In general, there is a spatially explicit pattern of phenology indicators from the North to the South in cities in the conterminous US, with an overall advanced SOS in the past three decades. The derived phenology product in the US urban domains at the national level is of great use for urban ecology studies for its

1

~~fine~~ medium spatial resolution (30 m) and long temporal span (30 years). The data are available at https://doi.org/10.6084/m9.figshare.7685645.

1 Introduction

Dynamics of vegetation phenology in urban ecosystems play an important role in influencing human activities such as energy

5   use and public health. The change of vegetation greening and dormancy affects various ecological and environmental processes, such as carbon storage, energy use, water cycle, and climate change (Zhou et al., 2016;Keenan et al., 2014;Peng et al., 2013;Tang et al., 2016). These influences are amplified in urban ecosystems due to the notably altered urban environment by anthropogenic activities. For example, the urban heat island (UHI) results in an earlier start and a longer duration of the growing season than surrounding rural areas (White et al., 2002;Zhang et al., 2004b;Jochner et al., 2011). The change of

10   vegetation phenology affects the start and duration of pollen season in urban domains, which has become a major concern by public health authorities for the potential risks of pollen-induced respiratory allergies (e.g., asthma) (Aas et al., 1997;Anenberg et al., 2017;Gong et al., 2012;Li et al., 2019b). Furthermore, the rapid pace of urbanization is expected to continue in the future, with more than 66% of the world's population residing in urban areas by 2050 (United Nations, 2018), which will result in a more notable effect of urban environment change. Also, changes in the urban environment due to atmospheric, soil, and light

15   pollutions will affect the plant phenology (e.g., leaf senescence) (Escobedo et al., 2011), resulting in different phenology characteristics in urban ecosystems. However, our knowledge about the vegetation phenology response to urbanization under different ~~development~~ urban morphology scenarios is still unclear, partly because of the difficulties in observing and mapping the dynamics of vegetation phenology at ~~fine~~ medium spatial and temporal resolutions in/around urban areas. Therefore, dynamics of vegetation phenology in urban domains is crucial for understanding the response of vegetation phenology to

20   urbanization, and this further helps to develop process-based phenology models for prediction under the compound effect of global warming and urbanization (Jochner and Menzel, 2015;Jochner et al., 2011;White et al., 2002).

Medium and coarse resolution satellite observations are inadequate to support vegetation phenology studies in urban domains, although they have been extensively used for phenology mapping. Relevant studies include using the advanced very high-resolution radiometer (AVHRR) data (Moody and Johnson, 2001;White et al., 2002;Piao et al., 2006;Cong et al., 2012), and

the moderate resolution imaging spectroradiometer (MODIS) data (Zhang et al., 2004b;Zhou et al., 2016;Walker et al., 2012;Walker et al., 2015;Liu et al., 2016). The primary advantage of these datasets is their long-term observations with a fine temporal resolution. However, the relatively coarse (1-8 km) spatial resolution is limited to capture the spatial heterogeneity of phenology in urban domains (White et al., 2002;Hogda et al., 2002). In contrast, Landsat observations with a ~~fine~~ medium

5   spatial resolution (30 m) and a long temporal span (since the 1980s) offer the opportunity to overcome this limitation (Zipper et al., 2016;Li et al., 2017b).

There are few attempts of mapping vegetation phenology in urban domains using Landsat observations at a ~~large~~ regional (or global) scale due to complex vegetation compositions in urban ecosystems and the ~~huge~~ large dataset required for analysis. Despite the high spatial resolution and long-term record of Landsat, the 16-days revisit frequency and the cloud contamination

10   ~~coverage~~ make it difficult to collect adequate observations to composite the time series of vegetation indices for investigating vegetation phenology dynamics. Therefore, the long-term mean pattern of vegetation phenology using multi-year observations were generally investigated in most Landsat-based phenology studies. After that, the annual variability of phenology indicators can be identified through measuring the difference of dates when the vegetation index in a specific year reaches the same magnitude as its long-term mean (Fisher et al., 2006;Melaas et al., 2013). However, currently this approach was mainly used

15   in natural ecosystems (e.g., deciduous forest) or at local scales (Fisher et al., 2006;Melaas et al., 2013;Li et al., 2017b).~~, and~~ Therefore, there lack large-scale applications in urban domains. First, vegetation types and compositions in urban ecosystems are more complicated, and the floral species are more abundant in cities than surrounding rural areas (Luz de la Maza et al., 2002). The seasonal pattern of vegetation growth varies among different vegetation types, which requires a more generalized approach to filter out available Landsat observations for a specific year to measure its gap to the long-term mean (Li et al.,

20   2017b). Second, an improved understanding of vegetation phenology in urban areas over different regions require massive Landsat observations and super-computational power. More than one thousand Landsat scenes need to process for mapping vegetation phenology dynamics in a given city, and this number is huge when expanding the mapping area at the national or global scales.

The advent of Google Earth Engine (GEE) platform provides the possibility to map vegetation phenology dynamics using the

25   long-term Landsat data at the regional and global scales. GEE is a start-of-art platform for planetary-scale data analysis,

3

mapping, and modelling, owing to free access to numerous global datasets and advanced computational capabilities (Gorelick et al., 2017). There are several successful studies built on the GEE platform for mapping long-term dynamics of forest and water, using all available Landsat images at the global scale (Hansen et al., 2013;Pekel et al., 2016). It is convenient to composite time series data of vegetation index at the pixel level on the GEE, using all clear-sky pixels. Also, the capability of

5   cloud-based computation offered by the GEE enables efficient and effective mapping practices at different spatial and temporal scales (Xiong et al., 2017).

To better support vegetation phenology studies in urban domains with ~~more~~ required spatiotemporal details, for the first time, we mapped annual vegetation phenology (1985-2015) using long-term Landsat observations at a high spatial resolution in the US and characterized the dynamics of urban vegetation phenology. The remainder of this paper describes the study area and

10 data (Section 2), the adopted method for mapping vegetation phenology indicators (Section 3), the results with discussion (Section 4), and concluding remarks (Section 5).

2 Study area and data

Our study area includes all ~~cities~~ urban areas greater than 500 km² and their surrounding rural areas in the conterminous US. First, the urban extent was derived from nighttime light (NTL) observations (2013) (Zhou et al., 2018;Zhou et al., 2014). Then,

15 a buffer zone with the same size as the urban area was identified as the surrounding rural area. The near equal size of urban and rural areas enables us to explore the response of vegetation phenology to urbanization through characterizing their phenology differences (Li et al., 2017a). In total, 148 urban clusters with different sizes were identified for deriving phenology indicators and their dynamics (Fig. S1).

Landsat surface reflectance data is ~~our~~ the primary dataset used for vegetation phenology mapping. Images obtained from

20 different sensors, i.e., Thematic Mapper (TM), Enhanced Thematic Mapper Plus (ETM+), and Operational Land Imager (OLI), were used to composite the time series of the enhanced vegetation index (EVI) of each pixel (Huete et al., 2002). The surface reflectance data have been corrected for the radiometric and~~,~~ topographic effects. ~~, and~~ The correction of atmospheric effect was performed using the Landsat ecosystem disturbance adaptive processing system (LEDAPS)~~s~~ (Masek et al., 2006), and ~~.~~

4

cClouds and shadows were removed using the function of mask procedure (Fmask) (Zhu and Woodcock, 2012) before compositing the EVI time series. Thus, all available clear-sky pixels during 1985-2015 were used in our analysis.

3 Method

We developed an automatic approach to map urban vegetation phenology indicators using long-term (1985-2015) Landsat images on the GEE platform (Fig. 1). First, we composited the EVI time series using all clear-sky observations at the pixel level, ordered by the day of year (DOY). A double logistic model was then applied on the derived EVI time series to obtain the long-term mean pattern of phenology indicators (start of season (SOS) and end of season (EOS) in Fig. 1a). Second, we derived the annual variability of phenology indicators in urban and surrounding rural areas (Fig. 1b), by measuring the difference of dates when the EVI in a specific year reaches the same magnitude as its long-term mean (Li et al., 2017b). Details of each step are presented in the following sections.

3.1 Long-term mean phenology indicators

We composited EVI observations over the years to reflect capture its seasonal change before the implementation of the double logistic model. First, we used all clear-sky observations of EVI and ordered them by their DOYs. This step allows us to retrieve the seasonal pattern of vegetation dynamics using multi-year data because the temporal distribution of Landsat data is uneven due to the satellite revisit time and sky conditions. Then, we applied a smoothing procedure using a moving average of continuous observations within 2 days to minimize the impact of abnormal observations. This procedure can keep the raw seasonal pattern of EVI (Fig. S2), and further helps to reduce the uncertainty of parameter estimation in the double logistic model.

We characterized the seasonal change of vegetation growth using a double logistic model. This model has several advantages when compared to other approaches such as the splines and harmonic models (Melaas et al., 2016b;Carrão et al., 2010): (1) it captures the green-up and senescence phases using different sigmoid functions; and (2) the physical meaning of parameters is related to the vegetation growth and senescence (Fisher et al., 2006;Li et al., 2017b). The derived EVI time series data were fitted using the double logistic model as Eq. 1.

$$f(t) = v_1 + v_2\left(\frac{1}{1+e^{-m_1(t-n_1)}} - \frac{1}{1+e^{-m_2(t-n_2)}}\right) \tag{1}$$

where $f(t)$ is the fitted EVI value at the day t; v_1 and v_2 are the background and amplitude of EVI over the entire year, respectively; and ~~and pair-parameters (i.e.,~~ m_1 & n_1, m_2 & n_2~~)~~ are the pair-parameters that capture the trends of green-up and senescence phases of vegetation growth, respectively. That is, n_1 and n_2 are dates ~~that~~with ~~have the~~ maximum increasing and decreasing rates of green-up and senescence in sigmoid curves~~, respectively, while~~and m_1 and m_2 ~~indicate their~~are the slopes that determine the shape of ~~two~~ sigmoid curves.

We developed a stepwise statistical approach to estimate the parameters of the double logistic model on the GEE platform for large-scale applications because currently the GEE platform does not support for optimization of parameters. Calculation of these parameters was presented in the Appendix. In general, the performance of this GEE-based double logistic model is robust for different land cover types, and the derived results are close to that from the optimization algorithm (Fig. 2). For example, although the magnitude of EVIs is relatively low in urban areas with low vegetation cover, a distinctive seasonal pattern of vegetation growth can be captured by the double logistic model. Also, sigmoid curves during green-up and senescence phrases are notably different across different vegetation cover types (e.g., forest and cropland). We evaluated the performance of the fitted double logistic model based on the correlation between the fitted and observed EVI observations. ~~to identify p~~Pixels ~~with experienced~~affected by land use/cover change during the study period or ~~pixels with~~havinge weak vegetation signals (e.g., ~~purely~~ extremely high built-up area or barren land) ~~always~~ could have~~result in~~ a lower fitting performance (e.g., correlation coefficient), ~~which~~and these pixels can be excluded for specific applications. A more detailed ~~introduction~~explanation of this procedure ~~can be referred to~~is reported in Li et al. (2017b). This stepwise statistical approach can be implemented at the pixel level on the GEE platform in a parallel manner, which significantly improved our mapping efficiency at the large scale.

We derived phenology indicators of SOS and EOS using ~~the~~a half-maximum criterion method (Fisher et al., 2006). ~~Based on this criterion~~In this method, SOS and EOS were ~~defined~~calculated as dates when the first derivative of EVI reaches the maximum increasing and decreasing rates during the green-up and senescence phases, respectively. Although there are other definitions of SOS and EOS such as inflection points (i.e., at the base of sigmoid curve) (Zhang et al., 2003), the criterion used in our study is ~~advantageous because: (1) they represent the dates when most leaves are likely to emerge (i.e., the steepest points on the symmetric sigmoid curves); and (2) they are~~ temporally more temporally stable and can be applied to plants

6

with different canopy structures (Fisher and Mustard, 2007). The growing season length (GSL) was defined as the difference between EOS and SOS.

3.2 Annual variability of phenology indicators

We derived the annual variability of vegetation phenology indicators using the developed generalized Landsat phenology (GLP) approach (Li et al., 2017b). Considering the temporally uneven distribution of available Landsat observations over the years, the annual variability of phenology indicators was measured as the difference of dates when the EVI in a specific year reaches the same magnitude as its long-term mean (Fisher et al., 2006;Melaas et al., 2013). Only EVI observations in the rational ranges of DOY and EVI (empty circles in shaded frames) in a given year were used in the GLP approach (Fig. 3). Observations outside this range (the shaded frames), which are either outliers or beyond the temporal ranges of green-up and senescence phases, were not used in calculating the annual variability. In the GLP approach, we also designed a self-adjusting strategy to derive the bounds of the shaded frames in the green-up and senescence phases (Fig. 3). For the green-up phase, the rational DOY ranges (two points on the long-term mean curve that intersected with the shaded green frame in Fig. 3) were defined as the dates when change rates (or derivative) of EVI reach the half-maximum before and after the date of SOS (i.e., the date with the maximum change rate). Thus, the corresponding EVI ranges were calculated based on the derived DOY ranges and the long-term mean curve. The rational ranges for the senescence phase were determined using the similar approach. This approach already showed its applications for different vegetation types (e.g., cropland or forest) with varying seasonal patterns of EVI. More details about this approach can be found in Li et al. (2017b).

4 Results and discussion

4.1 Performance of the GEE-based double logistic model

The performance of the developed GEE-based double logistic model is reasonably ~~well~~ good across different latitudes and ~~along the urban-rural gradient~~different vegetation cover types in urban ecosystems. Take forest as an example, the seasonal pattern of EVI varies from the South to the North in the US, with notably different sigmoid curves for the green-up and senescence phrases (Fig. 4). Our fitting approach can well capture the diverse seasonal patterns of EVI for forest across space. ~~Also~~ At the city scale, the proposed double logistic model shows a good performance of fitting EVI time series from urban to

7

rural areas ~~At local scale of urban ecosystem, the developed approach shows the good capability of fitting EVI time series along the urban rural gradient~~for different cover types from urban to rural areas (Fig. 5), where the vegetation composition and the seasonal pattern of EVI are more complicated compared to natural ecosystems. For sites in urban center, ~~although~~ despite their low value of EVIs ~~are low~~, a distinctive seasonal pattern of phenology is also captured by the proposed double logistic function, with a good fitting was observed.

4.2 Comparison with PhenoCam data

Overall, t~~T~~he derived phenology indicators (SOS and EOS) are spatially consistent with those from *in-situ* PhenoCam data at the large (e.g., national) scale ~~overall~~ (Fig. 6). PhenoCam is a regional-scale network of digital cameras that provide high temporal resolution vegetation canopy and phenology information (Richardson et al., 2018). The records in PhenoCam are observed green chromatic coordinate (GCC), which is used as the indicator of vegetation dynamics. We used all PhenoCam sites in the US and compared the mean SOS and EOS with Landsat derived results. The definition of SOS and EOS we used in the PhenoCam data (i.e., the half-maximum criterion) is consistent with our result derived from Landsat data. Overall, correlations of the derived SOS and EOS from the Landsat and PhenoCam are 0.66 and 0.43, respectively. Most indicators are around the 1:1 line, indicating a close correspondence of phenology indicators derived from these two independent datasets. For those sites (blue or light blue dots) with large differences, the performance of fitting ~~of~~ Landsat EVIs using the double logistic model is relatively ~~worse~~low because~~.~~ t~~T~~hese sites are mainly ~~distributed~~embedded in ecosystems that are dominated by shrubs, evergreen forests, or wetlands (Fig. S3). With correlation coefficients lower than 0.85 (worse fitting) excluded as suggested by Melaas et al. (2016b), the overall agreements between Landsat and PhenoCam derived results were notably improved to 0.86 and 0.94, for SOS and EOS, respectively. Discrepancies between these two sets of phenology indicators derived from Landsat and PhenoCam are mainly attributed to factors such as: (1) two different vegetation indices (i.e., EVI and GCC); and (2) the scale effect between *in-situ* PhenoCam and Landsat observations~~Discrepancies between these two sets of indicators derived from Landsat and PhenoCam are mainly attributed to two factors including: (1) using two different vegetation indices (i.e., EVI and GCC) (e.g., relatively weak EVI but strong GCC for sites in arid regions with sparse plants); and (2) the effect of field of view~~scale effect ~~for in-situ PhenoCam (e.g., species) and space-based Landsat observations (e.g., mixed vegetation types)~~ (Liu et al., 2017).

Overall, t~~T~~he annual variability of ~~phenology indicators (SOS and EOS)~~of SOS derived from Landsat observations ~~also shows a good agreement~~is consistent with that from the *in-situ* PhenoCam ~~results~~ observations (Fig. 7). We selected 11 deciduous broadleaf forest sites for comparison with continuous observations of more than five years (Fig. 7a). Landsat pixels located within 500 m of each PhenoCam station were used to ensure adequate samples to reflect the vegetation phenology dynamic at

5   the local scale for this comparison (Melaas et al., 2016a). The temporal dynamics of Landsat derived SOS and EOS generally follow the changes captured by PhenoCam observations (Fig. 7 b-c). A detailed illustration of the *Acadia* site indicates the SOS derived from the two datasets is notably decreasing during period 2006-2010 and their corresponding EOS is increasing after 2011. Although magnitudes of SOS and EOS are different over the years, their temporal trends (i.e., decreasing or increasing) are relatively consistent. The magnitude differences of SOS from Landsat and MODIS are likely attributed to scale

10   effects, which determines different phenology patterns within a particular remotely sensed pixel. Overall, the annual SOS indicator derived from Landsat shows a better agreement (0.74) with the result obtained from *in-situ* PhenoCam observations (Fig. 7d). The agreement of annual variability of Landsat and PhenoCam EOS is relatively weaker (0.26) (Fig. 7e), which is consistent with previous results reported by Melaas et al. (2016a). The main reason for the weak agreement of annual variability of EOS is the difference in greening represented by GCC and EVI. That is, in the green-up phase, both GCC and EVI are

15   rapidly increasing. While in the senescence phase, the EVI detected by Landsat slightly decreases, which is notably different from the pattern reflected by GCC that rapidly decreases once the leaf color changes.

4.3 Comparison with Harvard Forest phenology data

Our Landsat derived phenology indicators have a similar temporal pattern ~~also show a good agreement~~ with that from the Harvard Forest (HF) over the past decades (Fig. 8). The HF data were collected by field observers in spring and fall seasons

20   for more than 25 years (Richardson et al., 2006). Our Landsat derived indicators were compared with dates of SOS and EOS recorded in the HF data, in which SOS and EOS are defined as the dates when the leaf length reaches 50% of its final size and the leaf color reaches 10% of the color change to the greenest, respectively (Melaas et al., 2016a). Three dominant species of deciduous forest in the HF, ~~Three dominant species~~ including~~of~~ red oak (*Quercus rubra; QURU*), red maple (*Acer rubrum; ACRU*), and yellow birch (*Betula alleghaniensis; BEAL*) in the HF, were ~~included~~ used in our analysis.~~,~~ However, for other

25   vegetation types (e.g., evergreen forest), discernible phenology patterns can be also captured using the proposed methodology

9

(e.g. Fig. 4, Site 1)all of them belong to deciduous forest. Overall, the SOS of the three-dominant species in the HF is similar and shows has a good similar agreement temporal trend with SOS derived from Landsat observations (Fig. 8a). The RMSE between Landsat SOS and the HF data is 3.5 day, and the correlation coefficient is 0.81 (Fig. 8c), indicating a closer comparable SOS and a relatively consistent temporal pattern. EOS shows a relatively larger gap among species (Fig. 8b), i.e., the EOS of red oak is notably later compared to other two species of red maple and yellow birch. The Landsat derived EOS is within the range of EOS of the three species, and the temporal variability of two data sources are similar, although their magnitudes are different. The RMSE between Landsat EOS and the HF data is 3.7 day, and the correlation coefficient is 0.51 (Fig. 8d).

4.4 Comparison with MODIS data

Phenology indicators (e.g., SOS) derived from Landsat observations provide more spatial details in/around urban areas and are spatially consistent with those from MODIS (Fig. 9). Taking the Chicago metropolitan area as an example, we compared the Landsat derived SOS with that from MODIS in two ways. First, we estimated SOS from the MODIS EVI (16-day) using the same approach for Landsat. Second, we retrieved SOS from the widely used MODIS phenology product (MCD12Q2) (Zhang et al., 2003) for comparison with Landsat based SOS. It is worthy to note that the SOS defined in MCD12Q2 is the inflection point of EVI growth during the green-up phrase, and this definition is different from our half-maximum criterion (Fisher and Mustard, 2007). Therefore, the SOS of MCD12Q2 is generally earlier than the other two. Also, there are uncertainties in MCD12Q2 in highly urbanized regions, where the SOS is above 180 days (Fig. 9a). Overall, more spatial details of SOS can be revealed in results derived from Landsat compared to MODIS (Fig. 9b). In highly urbanized regions, Landsat SOS can also capture the seasonal pattern of vegetation growth. Normalized SOSs derived from MODIS and Landsat show a relatively consistent trend along the gradient of developed areas (Fig. 9c), although their magnitudes are different (Fig. 9a).

Landsat derived phenology indicator of SOS exhibits a consistent temporal pattern compared to MODIS with a longer temporal span (Fig. 10). Although the temporal distribution of Landsat is uneven compared to MODIS, the annual variability of phenology indicators can be captured well using the clear EVI observations in a given year relative to the long-term mean pattern. For example, there is a notable advancement of SOS in 2012, and all three SOSs captured this variability at the pixel and regional levels (Fig. 10a and 10b). The magnitude difference of derived SOS between Landsat and MCD12Q2 is mainly

due to their definitions, and the difference of SOS between Landsat and MODIS EVI is likely caused by scale effect (e.g., mixed pixels). It is worth noting that SOS derived from the half-maximum criterion in this study is consistently later compared to the MODIS product using the criterion of the inflection point~~In general, SOS derived from the criterion of half-maximum is larger than that from the criterion of the inflection point, which should be cautious when using this dataset.~~

4.5 Spatiotemporal patterns of phenology indicators

Phenology indicators (SOS, EOS, and GSL) in urban domains exhibit a spatially explicit pattern from the North to the South in the conterminous US, with an overall advanced SOS in the past three decades (Fig. 11). SOS becomes earlier and EOS becomes later along the latitudinal gradient, although such spatial difference is more discernible in SOS compared to EOS at the national scale. As a result, GSL shows a generally extended trend from the North to the South (Fig. 11a). This spatial pattern of phenology indicators (e.g., SOS) is also confirmed at the city level with more details (Fig. 11b), a major attribute of higher spatial resolution of Landsat data. Meanwhile, the SOS is advanced in the past three decades, particularly in cities in the northern US (e.g., Boston). Spatiotemporal patterns of phenology indicators in the conterminous US reflect the response of vegetation phenology to regional differences of elevation, temperature, precipitation, vegetation type, as well as the global warming in past decades (Zhang et al., 2004a;Li et al., 2017a). In addition, changes ~~of~~ in urban environment such as ~~such as~~ ~~the increment of~~ impervious surface, ~~and~~ air pollutions, ~~or~~and the species compositions can affect the spatiotemporal pattern of vegetation phenology in urban ecosystems (Li et al., 2015;Escobedo et al., 2011)~~, are correlated to the spatiotemporal pattern of vegetation phenology in urban ecosystems.~~

5 Data availability

The derived vegetation phenology data in urban domains are available at https://doi.org/10.6084/m9.figshare.7685645. (Li et al., 2019a).

6 Conclusions

This study generated the first national-scale dynamics of annual vegetation phenology in urban domains (all ~~cities~~ urban areas greater than 500 km^2 and their surrounding rural areas) using long-term (1985-2015) Landsat observations on the GEE

11

platform. First, we mapped the long-term mean seasonal pattern of vegetation dynamics using a double logistic model. In this step, we proposed a stepwise statistical approach to estimate parameters in the double logistic model and implemented it on the GEE platform. Next, we identified annual dynamics of phenology indicators (i.e., SOS and EOS) by measuring the difference of dates when the EVI in a specific year reaches the same magnitude as its long-term mean. Finally, we developed

5   the first ~~high~~ medium spatial resolution (30 m) phenology product in urban areas in the conterminous US, over past three decades (1985-2015).

Overall, t~~T~~he Landsat based phenology indicators ~~show good agreements~~agree with those derived from independent *in-situ* observations (PhenoCam and HF) and another widely used satellite observations from MODIS. Overall, the phenology indicators derived from Landsat and PhenoCam are consistent for their long-term mean and annual variability. The comparison

10   with field observations collected in the HF suggests the Landsat derived indicators can capture the temporal dynamics of vegetation phenology in this forest ecosystem. Besides, the Landsat derived phenology indicators can provide more spatial details in/around urban areas, compared to the moderate-resolution MODIS results. Also, the temporal trends of phenology indicator (e.g., SOS) derived from Landsat and MODIS are consistent overall, and Landsat additionally extends the temporal span than MODIS back to the past three decades.

15   The Landsat phenology product in urban areas is of great use in urban phenology studies such as phenology response to urbanization. There is a spatially explicit pattern of phenology indicators from the North to the South in US cities, with an overall advanced SOS in the past three decades. With this new phenology dataset (with a long temporal coverage and a high spatial resolution), the response of vegetation phenology to urbanization (e.g., UHI) can be further investigated, particularly for plants in the urban center or suburban areas with notably altered urban environment by anthropogenic activities, where

20   most people reside (Zhang et al., 2004b;Alberti et al., 2017). This dataset, together with ground-based pollen concentration data, is also of help in decision making relevant to pollen-induced allergy diseases (Li et al., 2019b). In addition, the derived leaf on/off information in this dataset is potentially useful for many vegetation-air pollution deposition models (Escobedo and Nowak, 2009). However, it is worth noting that this dataset is most applicable for deciduous forest type. For grassland and evergreen forests in tropical areas, the uncertainty could be high in the derived phenology indicators. In addition, our phenology

25   algorithm did not specifically consider pixels with land cover changes, which could be further improved when the product of

Appendix

5   The double logistic model used in the GLP approach includes two sigmoid curves indicating the green-up and senescence phases of vegetation growth (Eq. A1).

$$f(t) = v_1 + v_2 \left(\frac{1}{1+e^{-m_1(t-n_1)}} - \frac{1}{1+e^{-m_2(t-n_2)}} \right) \qquad \text{A1}$$

where $f(t)$ is the fitted EVI value at the day t; v_1 and v_2 are the background and amplitude of EVI over the entire year, respectively; the first sigmoid ($Sig_1: \frac{1}{1+e^{-m_1(t-n_1)}}$) with pair-parameters of m_1 & n_1 captures the green-up phase of vegetation

10   growth; and the second sigmoid ($Sig_2: \frac{1}{1+e^{-m_2(t-n_2)}}$) with pair-parameters of m_2 & n_2 captures the senescence phase of vegetation growth (Fig. A1).

We derived six parameters (i.e., v_1, v_2, m_1, n_1, m_2, and n_2) in the double logistic model using a statistics approach on the GEE platform. First, we estimated v_1 and v_2 based on the smoothed EVI time series, with abnormal observations (or noise) excluded. We calculated the quantile levels of 5th and 95th as the minimum v_1 and maximum EVI v_{max} over the entire DOY

15   range, to avoid possible biases caused by extreme values. Thus, v_2 can be determined as Eq. A2.

$$v_2 = v_{max} - v_1 \qquad \text{A2}$$

The first part (Sig_1) of the double logistic model in the green-up phase (Eq. A3) can be translated to Eq. A4 by using the smoothed EVI time series only during the green-up phase before doy_{max} and converted into a logarithmic form as Eq. A5.

$$Sig_1 = \frac{f(t)-v_1}{v_2} = \frac{1}{1+e^{-m_1(t-n_1)}} \qquad \text{A3}$$

20

$$\frac{v_1+v_2-f(t)}{f(t)-v_1} = e^{-m_1(t-n_1)} \qquad \text{A4}$$

$$\ln\left(\frac{v_1+v_2-f(t)}{f(t)-v_1}\right) = -m_1(t-n_1) \qquad \text{A5}$$

13

where the left term in Eq. A5 can be calculated using v_1 and v_2, together with the smoothed EVI time series $f(t)$ only during the green-up phase before doy_{max}. m_1 and n_1 can be estimated using the least square regression approach.

Finally, based on the estimated parameters (i.e., v_1, v_2, m_1 and n_1), the second part (Sig_2) of the double logistic model in the senescence phase can be formulated as Eqs. A6-8, respectively. In a similar manner, the pair-parameters of m_2 and n_2 can be estimated using the least square regression approach, together with the smoothed EVI time series during the green-up and senescence phases together.

$$Sig_2 = \frac{v_1 + v_2 Sig_1 - f(t)}{v2} = \frac{1}{1 + e^{-m_2(t - n_2)}} \qquad \text{A6}$$

$$\frac{v_2(1 - Sig_1) - v_1 + f(t)}{v_1 + v_2 Sig_1 - f(t)} = e^{-m_2(t - n_2)} \qquad \text{A7}$$

$$\ln\left(\frac{v_2(1 - Sig_1) - v_1 + f(t)}{v_1 + v_2 Sig_1 - f(t)}\right) = -m_2(t - n_2) \qquad \text{A8}$$

Author contributions

ZY and LX designed the research; LX and ZY implemented the research and wrote the paper; GA, ML, LC, and WQ edited and revised the manuscript.

Competing interests

The authors declare that they have no conflict of interest.

Acknowledgments

References

Aas, K., Aberg, N., Bachert, C., Bergmann, K., Bergmann, R., and Bonini, S.: Allergic disease as a public health problem in Europe, European allergy, 1-46, 1997.
Alberti, M., Correa, C., Marzluff, J. M., Hendry, A. P., Palkovacs, E. P., Gotanda, K. M., Hunt, V. M., Apgar, T. M., and Zhou, Y.: Global urban signatures of phenotypic change in animal and plant populations, P Natl Acad Sci USA, 114, 8951-8956, 10.1073/pnas.1606034114, 2017.
Anenberg, S. C., Weinberger, K. R., Roman, H., Neumann, J. E., Crimmins, A., Fann, N., Martinich, J., and Kinney, P. L.: Impacts of oak pollen on allergic asthma in the United States and potential influence of future climate change, GeoHealth, 1, 80-92, 2017.

Carrão, H., Gonçalves, P., and Caetano, M.: A nonlinear harmonic model for fitting satellite image time series: Analysis and prediction of land cover dynamics, IEEE Transactions on Geoscience and Remote Sensing, 48, 1919-1930, 2010.

Cong, N., Piao, S., Chen, A., Wang, X., Lin, X., Chen, S., Han, S., Zhou, G., and Zhang, X.: Spring vegetation green-up date in China inferred from SPOT NDVI data: A multiple model analysis, Agricultural and Forest Meteorology, 165, 104-113, http://dx.doi.org/10.1016/j.agrformet.2012.06.009, 2012.

Escobedo, F. J., and Nowak, D. J.: Spatial heterogeneity and air pollution removal by an urban forest, Landscape Urban Plan, 90, 102-110, 2009.

Escobedo, F. J., Kroeger, T., and Wagner, J. E.: Urban forests and pollution mitigation: Analyzing ecosystem services and disservices, Environmental pollution, 159, 2078-2087, 2011.

Fisher, J. I., Mustard, J. F., and Vadeboncoeur, M. A.: Green leaf phenology at Landsat resolution: Scaling from the field to the satellite, Remote Sens Environ, 100, 265-279, http://dx.doi.org/10.1016/j.rse.2005.10.022, 2006.

Fisher, J. I., and Mustard, J. F.: Cross-scalar satellite phenology from ground, Landsat, and MODIS data, Remote Sens Environ, 109, 261-273, http://dx.doi.org/10.1016/j.rse.2007.01.004, 2007.

Gong, P., Liang, S., Carlton, E. J., Jiang, Q., Wu, J., Wang, L., and Remais, J. V.: Urbanisation and health in China, Lancet, 379, 843-852, http://dx.doi.org/10.1016/S0140-6736(11)61878-3, 2012.

Gorelick, N., Hancher, M., Dixon, M., Ilyushchenko, S., Thau, D., and Moore, R.: Google Earth Engine: Planetary-scale geospatial analysis for everyone, Remote Sens Environ, 202, 18-27, http://dx.doi.org/10.1016/j.rse.2017.06.031, 2017.

Hansen, M. C., Potapov, P. V., Moore, R., Hancher, M., Turubanova, S. A., Tyukavina, A., Thau, D., Stehman, S. V., Goetz, S. J., Loveland, T. R., Kommareddy, A., Egorov, A., Chini, L., Justice, C. O., and Townshend, J. R. G.: High-Resolution Global Maps of 21st-Century Forest Cover Change, Science, 342, 850-853, 10.1126/science.1244693, 2013.

Hogda, K. A., Karlsen, S. R., Solheim, I., Tommervik, H., and Ramfjord, H.: The start dates of birch pollen seasons in Fennoscandia studied by NOAA AVHRR NDVI data, Geoscience and Remote Sensing Symposium, 2002. IGARSS'02. 2002 IEEE International, 2002, 3299-3301,

Huete, A., Didan, K., Miura, T., Rodriguez, E. P., Gao, X., and Ferreira, L. G.: Overview of the radiometric and biophysical performance of the MODIS vegetation indices, Remote Sens Environ, 83, 195-213, http://dx.doi.org/10.1016/S0034-4257(02)00096-2, 2002.

Jochner, S., and Menzel, A.: Urban phenological studies – Past, present, future, Environmental Pollution, 203, 250-261, http://dx.doi.org/10.1016/j.envpol.2015.01.003, 2015.

Jochner, S. C., Sparks, T. H., Estrella, N., and Menzel, A.: The influence of altitude and urbanisation on trends and mean dates in phenology (1980–2009), International Journal of Biometeorology, 56, 387-394, 10.1007/s00484-011-0444-3, 2011.

Keenan, T. F., Gray, J., Friedl, M. A., Toomey, M., Bohrer, G., Hollinger, D. Y., Munger, J. W., O/'Keefe, J., Schmid, H. P., Wing, I. S., Yang, B., and Richardson, A. D.: Net carbon uptake has increased through warming-induced changes in temperate forest phenology, Nature Clim. Change, 4, 598-604, 10.1038/nclimate2253
http://www.nature.com/nclimate/journal/v4/n7/abs/nclimate2253.html#supplementary-information, 2014.

Li, X., Gong, P., and Liang, L.: A 30-year (1984–2013) record of annual urban dynamics of Beijing City derived from Landsat data, Remote Sens Environ, 166, 78-90, 10.1016/j.rse.2015.06.007, 2015.

Li, X., Zhou, Y., Asrar, G. R., Mao, J., Li, X., and Li, W.: Response of vegetation phenology to urbanization in the conterminous United States, Global Change Biology, 23, 6030-6046, 10.1111/gcb.13562, 2017a.

Li, X., Zhou, Y., Asrar, G. R., and Meng, L.: Characterizing spatiotemporal dynamics in phenology of urban ecosystems based on Landsat data, Science of The Total Environment, 605–606, 721-734, https://doi.org/10.1016/j.scitotenv.2017.06.245, 2017b.

Li, X., Zhou, Y., Meng, L., Asrar, G., Lu, C., and Wu, Q.: A dataset of 30-meter annual vegetation phenology indicators (1985-2015) in urban areas of the conterminous United States, 2019a.

Li, X., Zhou, Y., Meng, L., Asrar, G. R., Sapkota, A., and Coates, F.: Characterizing the relationship between satellite phenology and pollen season: a case study of birch, Remote Sens Environ, 222, 257-274, j.rse.2018.12.036, 2019b.

Liu, Y., Wu, C., Peng, D., Xu, S., Gonsamo, A., Jassal, R. S., Altaf Arain, M., Lu, L., Fang, B., and Chen, J. M.: Improved modeling of land surface phenology using MODIS land surface reflectance and temperature at evergreen needleleaf forests of central North America, Remote Sens Environ, 176, 152-162, http://dx.doi.org/10.1016/j.rse.2016.01.021, 2016.

Liu, Y., Hill, M. J., Zhang, X., Wang, Z., Richardson, A. D., Hufkens, K., Filippa, G., Baldocchi, D. D., Ma, S., Verfaillie, J., and Schaaf, C. B.: Using data from Landsat, MODIS, VIIRS and PhenoCams to monitor the phenology of California oak/grass savanna and open grassland across spatial scales, Agricultural and Forest Meteorology, 237-238, 311-325, https://doi.org/10.1016/j.agrformet.2017.02.026, 2017.

Luz de la Maza, C., Hernández, J., Bown, H., Rodríguez, M., and Escobedo, F.: Vegetation diversity in the Santiago de Chile urban ecosystem, Arboricultural journal, 26, 347-357, 2002.

Masek, J. G., Vermote, E. F., Saleous, N. E., Wolfe, R., Hall, F. G., Huemmrich, K. F., Gao, F., Kutler, J., and Lim, T.-K.: A Landsat surface reflectance dataset for North America, 1990-2000, Geoscience and Remote Sensing Letters, IEEE, 3, 68-72, 2006.

Melaas, E. K., Friedl, M. A., and Zhu, Z.: Detecting interannual variation in deciduous broadleaf forest phenology using Landsat TM/ETM + data, Remote Sens Environ, 132, 176-185, http://dx.doi.org/10.1016/j.rse.2013.01.011, 2013.

15

Melaas, E. K., Sulla-Menashe, D., Gray, J. M., Black, T. A., Morin, T. H., Richardson, A. D., and Friedl, M. A.: Multisite analysis of land surface phenology in North American temperate and boreal deciduous forests from Landsat, Remote Sens Environ, 186, 452-464, http://dx.doi.org/10.1016/j.rse.2016.09.014, 2016a.

Melaas, E. K., Wang, J. A., Miller, D. L., and Friedl, M. A.: Interactions between urban vegetation and surface urban heat islands: a case study in the Boston metropolitan region, Environmental Research Letters, 11, 054020, 2016b.

Moody, A., and Johnson, D. M.: Land-surface phenologies from AVHRR using the discrete Fourier transform, Remote Sens Environ, 75, 305-323, 2001.

Pekel, J.-F., Cottam, A., Gorelick, N., and Belward, A. S.: High-resolution mapping of global surface water and its long-term changes, Nature, 540, 418-422, 10.1038/nature20584

http://www.nature.com/nature/journal/v540/n7633/abs/nature20584.html#supplementary-information, 2016.

Peng, S., Piao, S., Ciais, P., Myneni, R. B., Chen, A., Chevallier, F., Dolman, A. J., Janssens, I. A., Penuelas, J., Zhang, G., Vicca, S., Wan, S., Wang, S., and Zeng, H.: Asymmetric effects of daytime and night-time warming on Northern Hemisphere vegetation, Nature, 501, 88-92, 10.1038/nature12434

http://www.nature.com/nature/journal/v501/n7465/abs/nature12434.html#supplementary-information, 2013.

Piao, S., Fang, J., Zhou, L., Ciais, P., and Zhu, B.: Variations in satellite-derived phenology in China's temperate vegetation, Global Change Biology, 12, 672-685, 10.1111/j.1365-2486.2006.01123.x, 2006.

Richardson, A. D., Bailey, A. S., Denny, E. G., Martin, C. W., and O'KEEFE, J.: Phenology of a northern hardwood forest canopy, Global Change Biology, 12, 1174-1188, 2006.

Richardson, A. D., Hufkens, K., Milliman, T., Aubrecht, D. M., Chen, M., Gray, J. M., Johnston, M. R., Keenan, T. F., Klosterman, S. T., and Kosmala, M.: Tracking vegetation phenology across diverse North American biomes using PhenoCam imagery, Scientific data, 5, 180028, 2018.

Tang, J., Körner, C., Muraoka, H., Piao, S., Shen, M., Thackeray, S. J., and Yang, X.: Emerging opportunities and challenges in phenology: a review, Ecosphere, 7, 1-17, 10.1002/ecs2.1436, 2016.

United Nations: World urbanization prospects: the 2018 revision, UN, 2018.

Walker, J. J., de Beurs, K. M., Wynne, R. H., and Gao, F.: Evaluation of Landsat and MODIS data fusion products for analysis of dryland forest phenology, Remote Sens Environ, 117, 381-393, http://dx.doi.org/10.1016/j.rse.2011.10.014, 2012.

Walker, J. J., de Beurs, K. M., and Henebry, G. M.: Land surface phenology along urban to rural gradients in the U.S. Great Plains, Remote Sens Environ, 165, 42-52, http://dx.doi.org/10.1016/j.rse.2015.04.019, 2015.

White, A. M., Nemani, R. R., Thornton, E. P., and Running, W. S.: Satellite Evidence of Phenological Differences Between Urbanized and Rural Areas of the Eastern United States Deciduous Broadleaf Forest, Ecosystems, 5, 260-273, 10.1007/s10021-001-0070-8, 2002.

Xiong, J., Thenkabail, P., Tilton, J., Gumma, M., Teluguntla, P., Oliphant, A., Congalton, R., Yadav, K., and Gorelick, N.: Nominal 30-m Cropland Extent Map of Continental Africa by Integrating Pixel-Based and Object-Based Algorithms Using Sentinel-2 and Landsat-8 Data on Google Earth Engine, Remote Sensing, 9, 1065, 2017.

Zhang, X., Friedl, M. A., Schaaf, C. B., Strahler, A. H., Hodges, J. C. F., Gao, F., Reed, B. C., and Huete, A.: Monitoring vegetation phenology using MODIS, Remote Sens Environ, 84, 471-475, http://dx.doi.org/10.1016/S0034-4257(02)00135-9, 2003.

Zhang, X., Friedl, M. A., Schaaf, C. B., and Strahler, A. H.: Climate controls on vegetation phenological patterns in northern mid-and high latitudes inferred from MODIS data, Global Change Biology, 10, 1133-1145, 2004a.

Zhang, X., Friedl, M. A., Schaaf, C. B., Strahler, A. H., and Schneider, A.: The footprint of urban climates on vegetation phenology, Geophysical Research Letters, 31, L12209, 10.1029/2004GL020137, 2004b.

Zhou, D., Zhao, S., Zhang, L., and Liu, S.: Remotely sensed assessment of urbanization effects on vegetation phenology in China's 32 major cities, Remote Sens Environ, 176, 272-281, http://dx.doi.org/10.1016/j.rse.2016.02.010, 2016.

Zhou, Y., Smith, S. J., Elvidge, C. D., Zhao, K., Thomson, A., and Imhoff, M.: A cluster-based method to map urban area from DMSP/OLS nightlights, Remote Sens Environ, 147, 173-185, 10.1016/j.rse.2014.03.004, 2014.

Zhou, Y., Li, X., Asrar, G. R., Smith, S. J., and Imhoff, M.: A global record of annual urban dynamics (1992-2013) from nighttime lights, Remote Sens Environ, 219, 206-220, 2018.

Zhu, Z., and Woodcock, C. E.: Object-based cloud and cloud shadow detection in Landsat imagery, Remote Sens Environ, 118, 83-94, http://dx.doi.org/10.1016/j.rse.2011.10.028, 2012.

Zipper, S. C., Schatz, J., Singh, A., Kucharik, C. J., Townsend, P. A., and Loheide, I., Steven P. : Urban heat island impacts on plant phenology: intra-urban variability and response to land cover, Environmental Research Letters, 11, 054023, 2016.

16
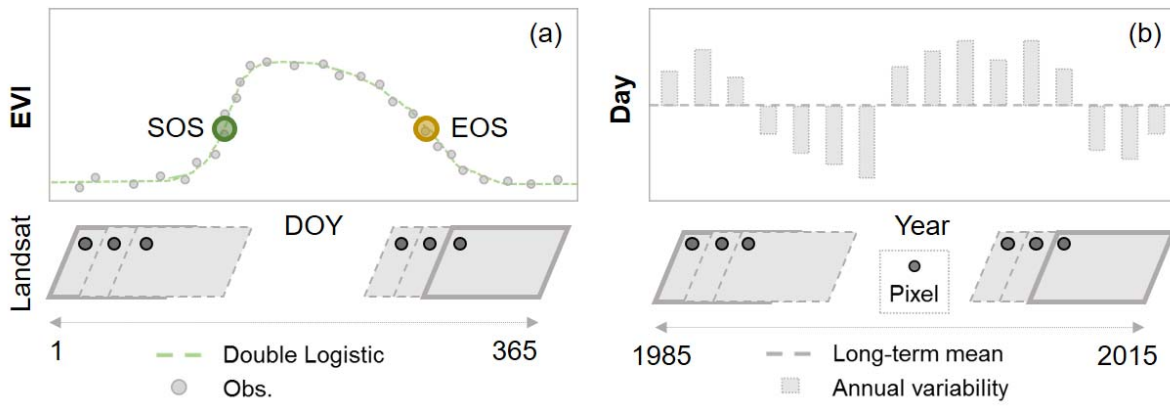
Fig. 1: The proposed framework for deriving long-term (1985-2015) mean vegetation phenology indicators (start of season-SOS -and end of season - EOS) (a) and their annual variabilities (b).
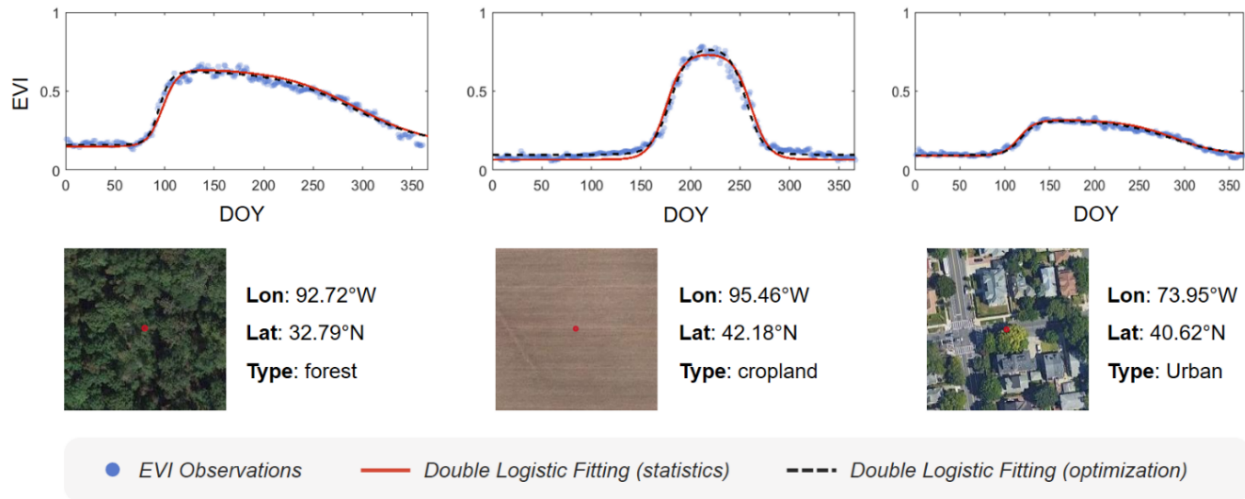
Fig. 2: Seasonal patterns of vegetation growth captured by the double logistic model for three distinctly different land cover types. The extent of a snapshot is 100m × 100m, and the red dot in the snapshot is the location of the Enhanced Vegetation Index (EVI) plot. EVI observations were composited using all clear-sky pixels during the past three decades (1985-2015).
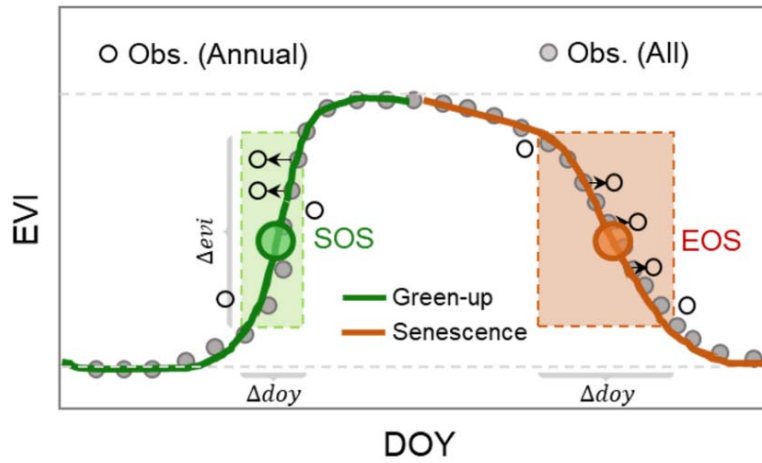
Fig. 3: Illustration of the generalized Landsat phenology (GLP) approach for identifying the annual variability of phenology indicators. The solid circles are long-term enhanced vegetation index (EVI) observations and the empty circles are observations at a specific year. The shaded frames colored as green and brown are the rational ranges of day of year (DOY) and EVI to be used during the green-up and senescence phases, respectively.

19
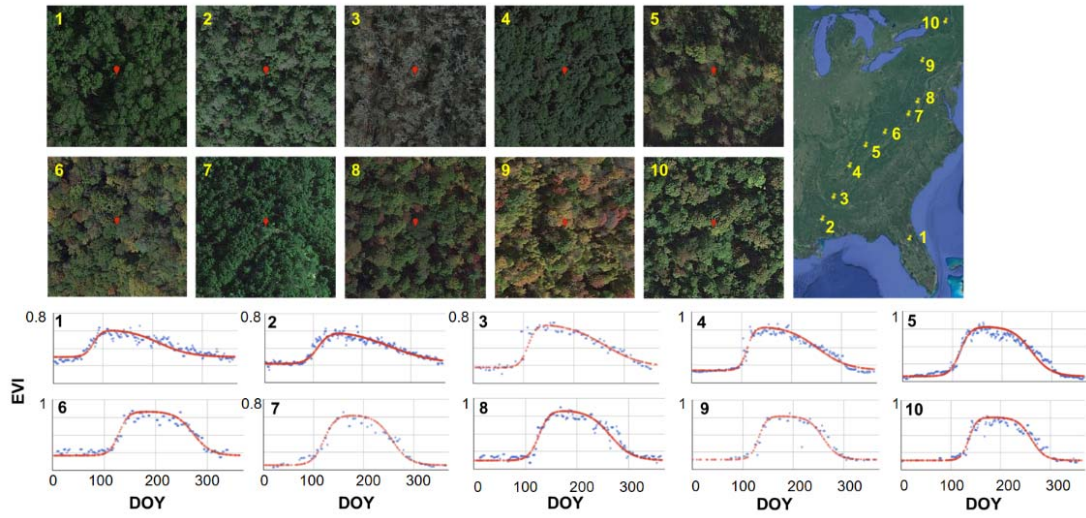
Fig. 4: Performance of the Google Earth Engine (GEE)-based double logistic model from the South to the North in the US United States using forest as an example. Each snapshot indicates a 1km² square, and the red dot in the middle is the location (30m) of the enhanced vegetation index (EVI) time series fitting.
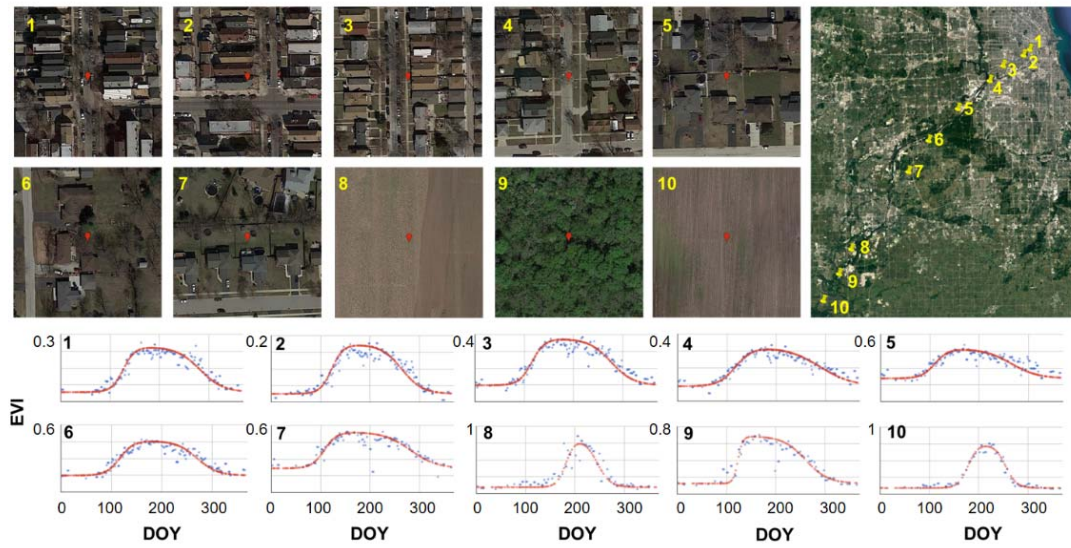
**Fig. 5:** Performance of the Google Earth Engine (GEE)-based double logistic model for sites along an example urban-rural gradientfrom urban center to rural areas in the Chicago metropolitan area. Each snapshot indicates a 1km² square, and the red dot in the middle is the location (30m) of the enhanced vegetation index (EVI) time series fitting.

21
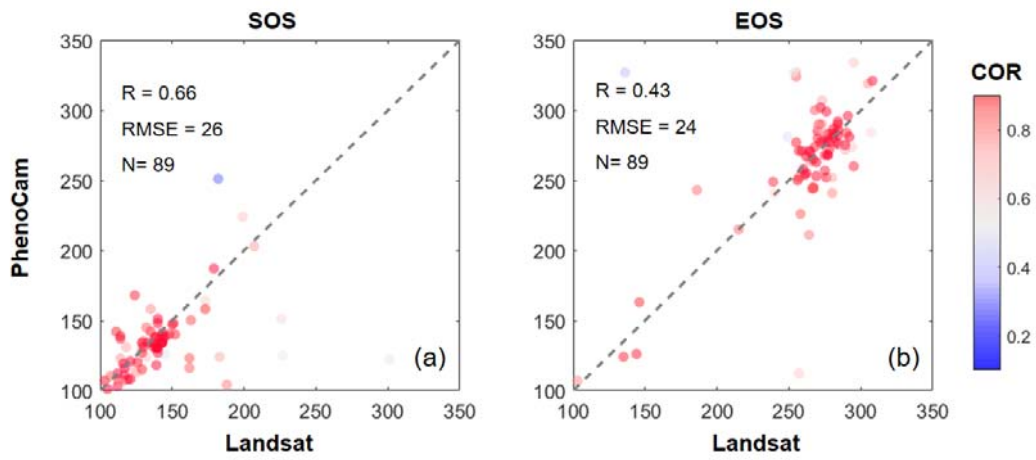
Fig. 6: Comparison of the period (2001-2015) mean phenology indicators of the start of season (SOS) (a) and the end of season (EOS) (b) derived from Landsat and PhenoCam observations. COR: the correlation coefficient between the raw and fitted EVIs using the double logistic model.

22
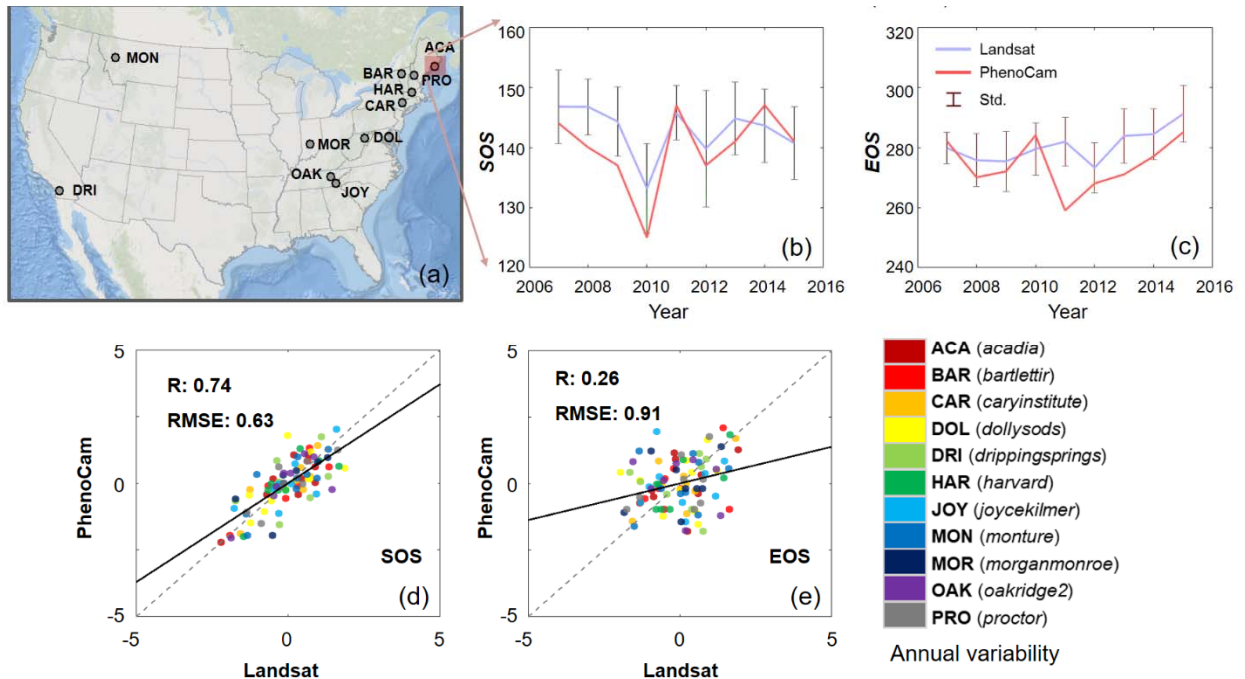
Fig. 7: Selected PhenoCam sites of deciduous broadleaf forest (a). Annual time series of phenology indicators in the station of *Acadia* for the start of season (SOS) (b) and the end of season (EOS) (c). Comparison of annual variability of SOS (d) and EOS (e) between Landsat and PhenoCam phenology indicators across all stations. The annual variability for each site is defined as $(x - \mu)/\sigma$, where x is the annual value of SOS and EOS, μ and σ are mean and standard deviation of SOS or EOS over the years.

23
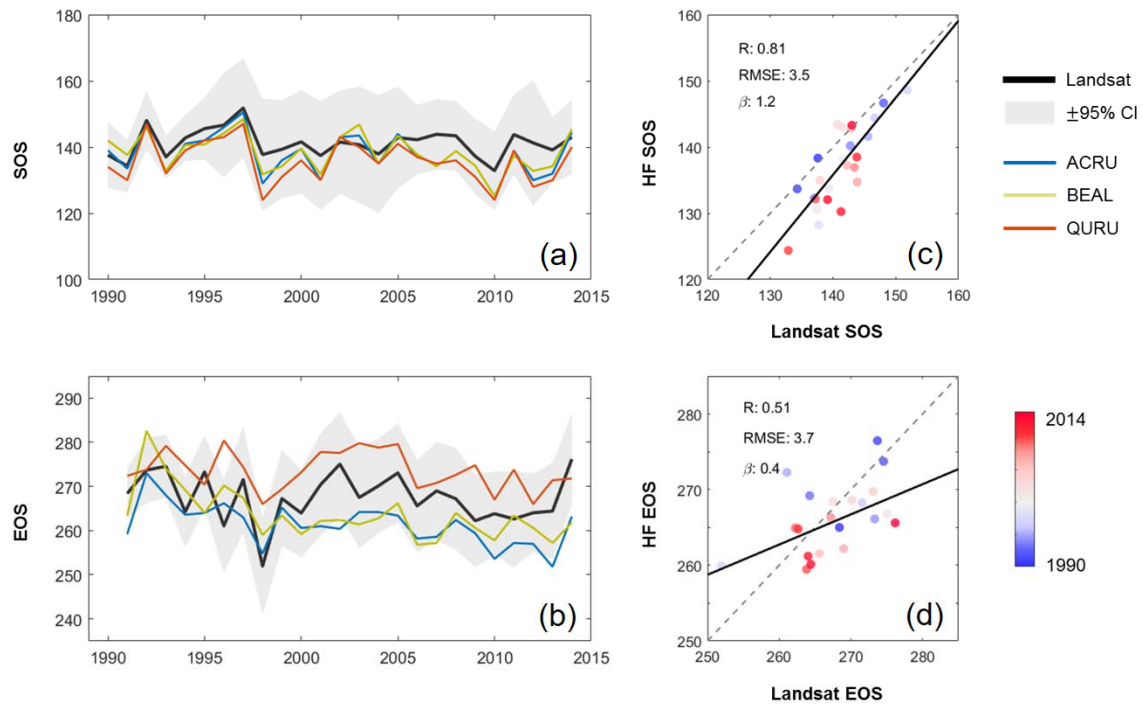
Fig. 8: Annual dynamics of the start of season (SOS) (a) and the end of season (EOS) (b) derived from Landsat and Harvard Forest (HF) observations and their scatter plots of SOS (c) and EOS (d) over the years.
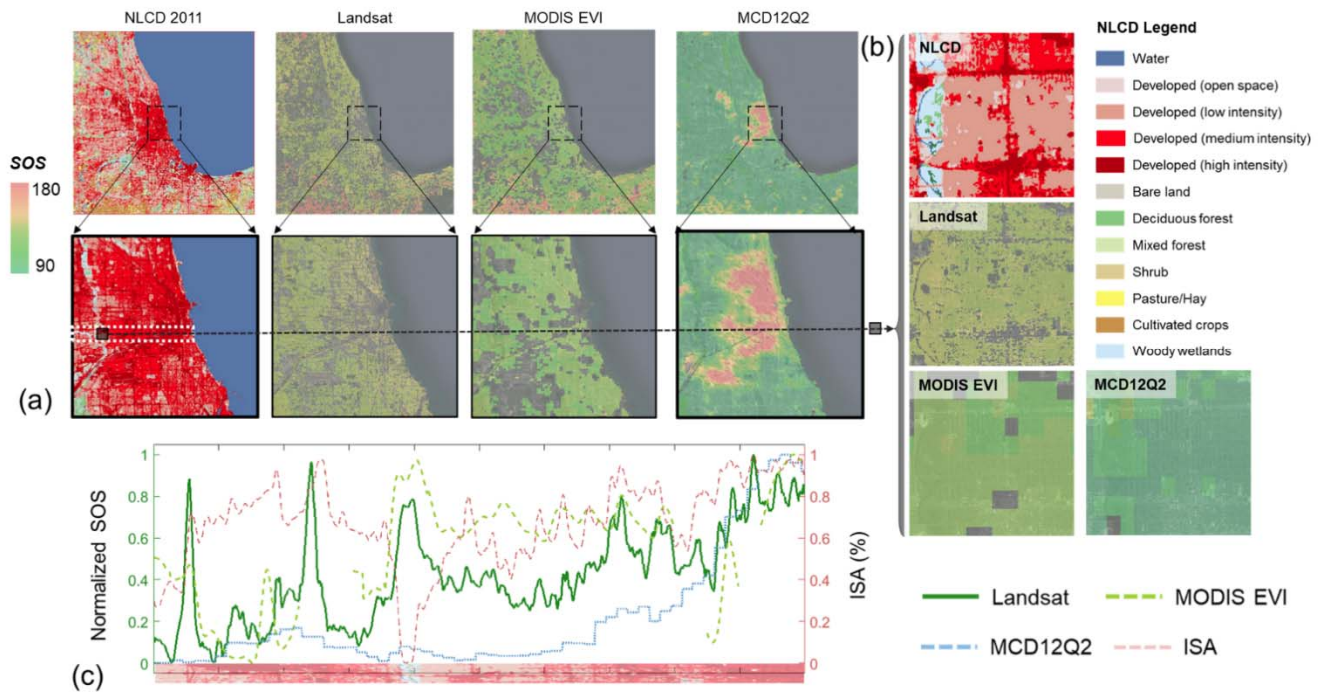
Fig. 9: Spatial patterns of the mean start of season (SOS) (2001-2014) derived from Landsat, the Moderate Resolution Imaging Spectroradiometer (MODIS) enhanced vegetation index (-EVI), and MCD12Q2 and the land cover from the national land cover database (NLCD) (2011) in the Chicago metropolitan area (a). Enlarged views (b) at the location of the black square in (a). Change of normalized SOS and impervious surface area (ISA) (c) along the white rectangle in (a) (from left to right). Pixels without good fitting performance (i.e., the correlation coefficient is lower than 0.85) were removed in the derived SOS from Landsat and MODIS EVI.
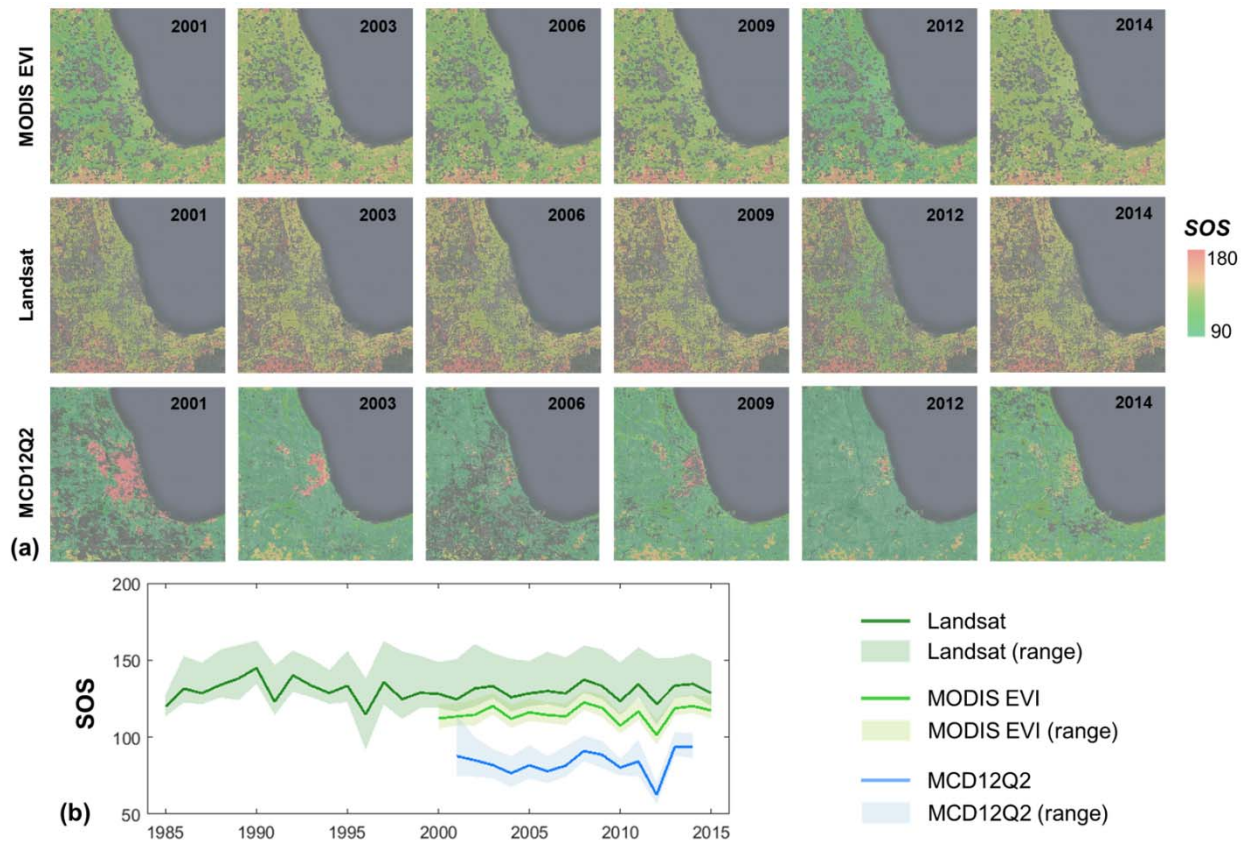
Fig. 10: Annual start of season (SOS) derived from Landsat, the Moderate Resolution Imaging Spectroradiometer (MODIS) enhanced vegetation index (EVI), and MCD12Q2 in the Chicago metropolitan area in representative years (a) and the temporal trend at the regional level (b). Solid lines are the mean SOSs at the regional level and shadowed frames indicate the range of SOS within the 25th and 75th quantile levels. Pixels without good fitting performance (i.e., the correlation coefficient is lower than 0.85) were removed in the derived SOS from Landsat and MODIS EVI.

26
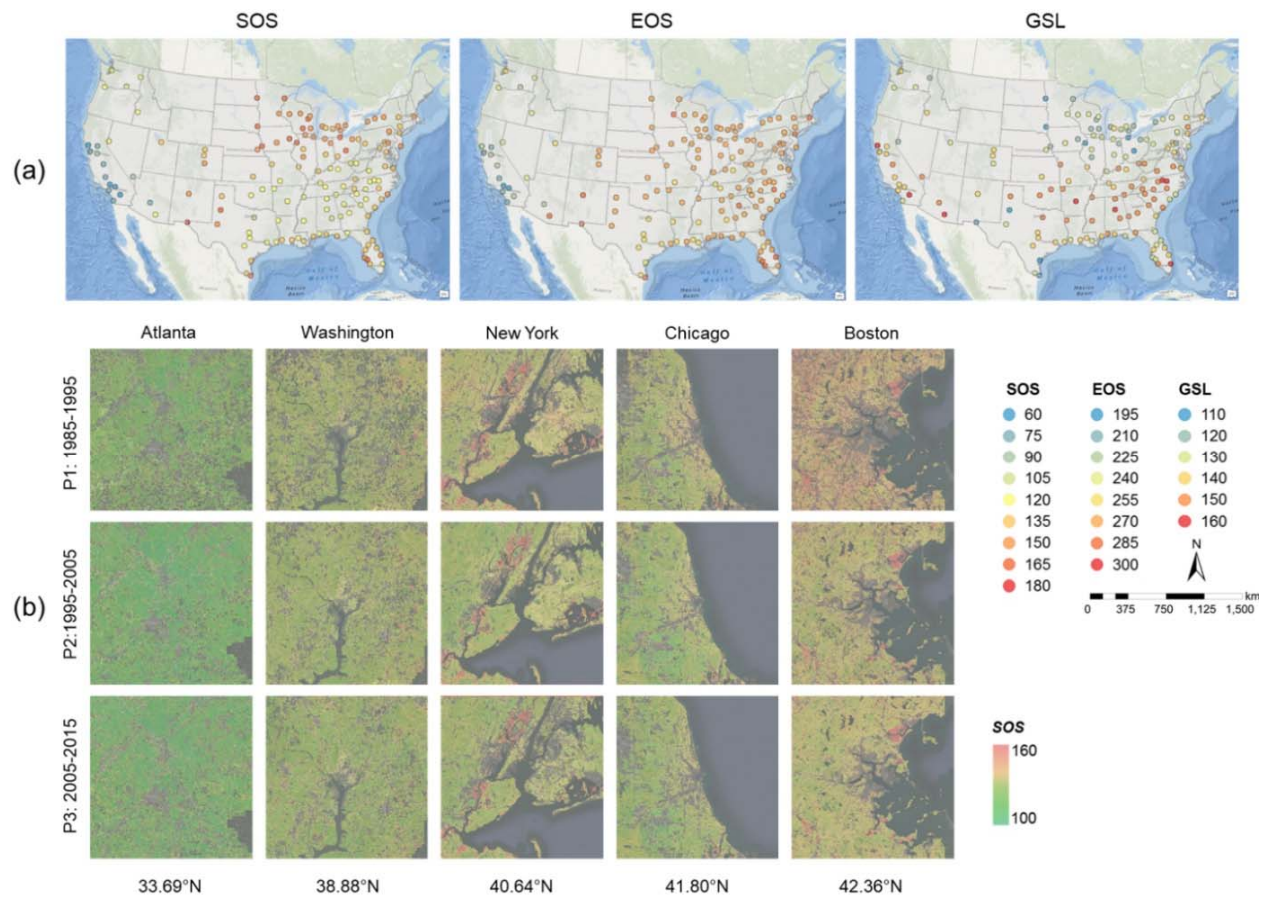
Fig. 11: Spatial patterns of the mean (1985-2015) vegetation phenology indicators (start of season - SOS, end of season - EOS, and growth season length - GSL) in the ~~US~~ United States cities (a) and SOS in representative cities in the past three decades (b). Each dot in (a) represents the center of the urban cluster, and the spatial extent of selected cities in (b) is 25 km × 25 km.
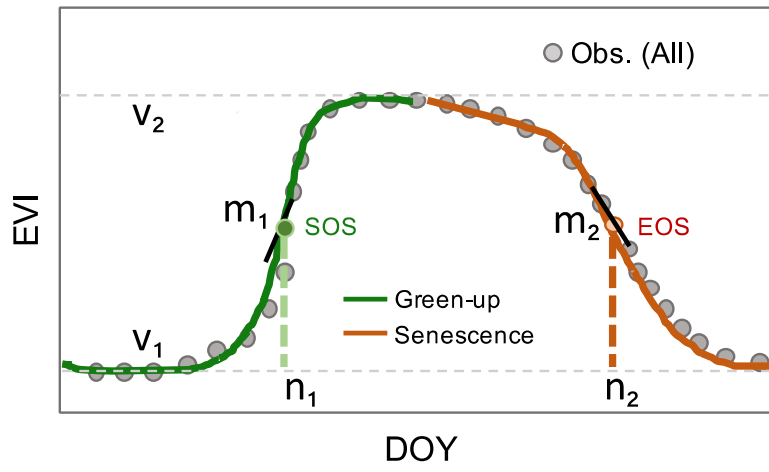
Fig. A1: Illustration of the double logistic model and corresponding parameters. EVI: enhanced vegetation index; DOY: day of year.